Planar Visualisation of Vortical Flows

R. D. Knowles*   M. V. Finnis   A. J. Saddington   K. Knowles

Department of Aerospace, Power and Sensors

Cranfield University, Defence Academy of the United Kingdom

Shrivenham, Swindon, SN6 8LA

Abstract

This paper presents two over-looked post-processing techniques which provide the investigator with additional tools for data analysis and visualisation. Both techniques exploit the trend for planar experimental data collection and are implemented in two-dimensions. Critically, both techniques are suitable for use on computational and experimental datasets, require no a-priori knowledge of the flow-field and minimal user interaction during processing. Firstly, line integral convolution will be introduced as an alternative to streamline or in-plane velocity vector visualisation. Secondly, a feature identification procedure will be outlined that can be used to reduce datasets for clearer visualisation and provide quantitative information about topological flow features.

Keywords: line-integral convolution, vortex identification, critical-point analysis, visualisation

1   Introduction

The study of separated flows relies heavily upon understanding the behaviour of wake vortices. Capturing vortex structures has been the focus of many experimental and computational endeavours. In the experimental arena the maturation of non-intrusive laser-based measurement techniques has led to an extended database from which computational models can be verified and validated. The majority of laser-based experimental investigations revolve around gathering selected planes of information rather than volume mapping. These planes, often perpendicular to the vortices of interest, range from

---

*Now with Advantage CFD, Reynard Park, Brackley, Northamptonshire, NN13 7RP

flow visualisation to unsteady, three-dimensional velocities. Equivalent planes can be extracted from the computational domain and directly compared. It was deemed essential, therefore, that any novel post-processing techniques could be implemented in two-dimensions and should be equally suited to experimental and computational datasets.

Figure 1 presents some of the commonly used post-processing techniques as applied to the instantaneous wake behind a two-dimensional cylinder. All the techniques are intuitive and easily understood although each have limitations which are visible in the figure.

(a) Velocity vectors.

(b) Vorticity.

(c) Streamlines – upstream rake.

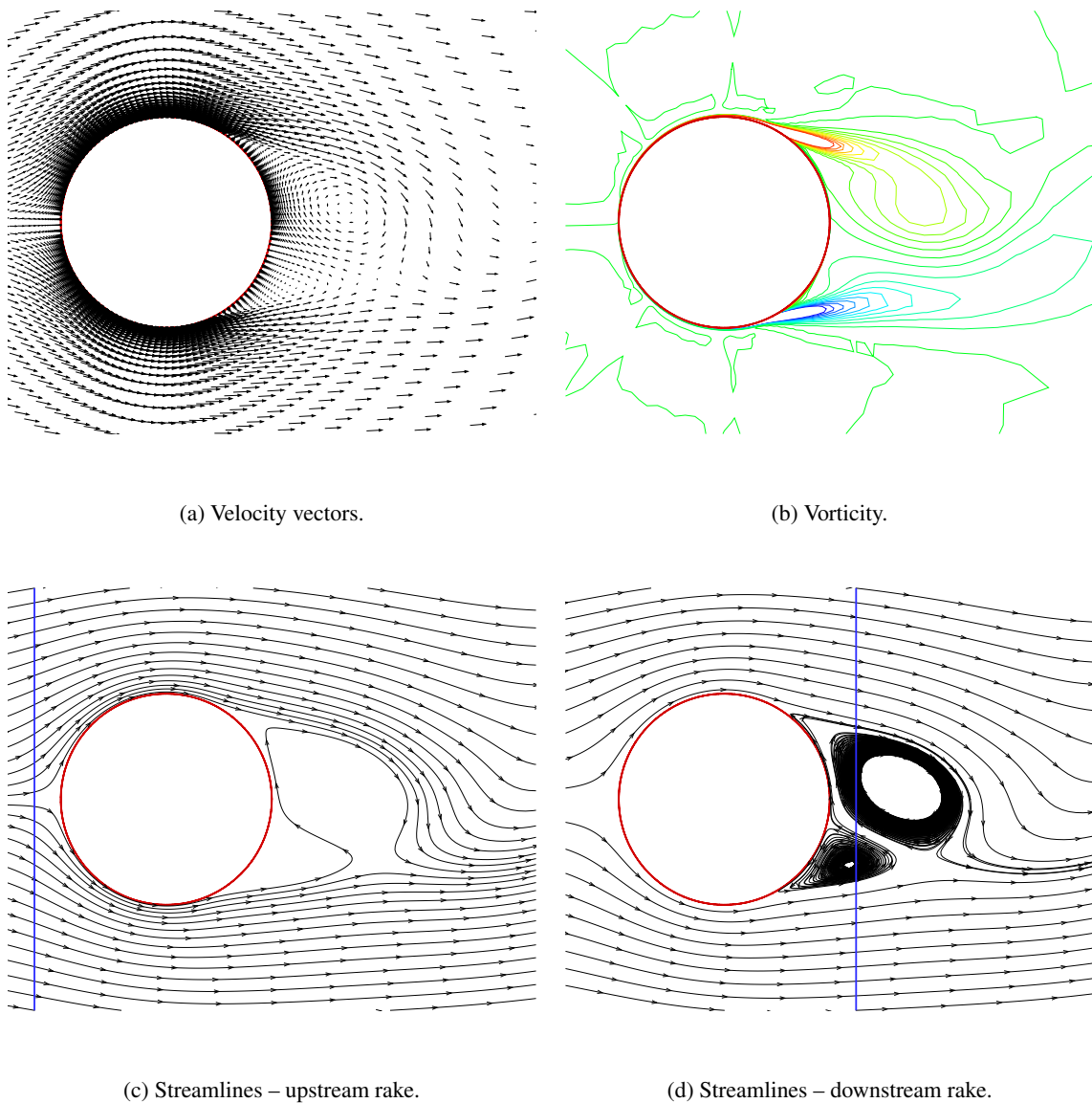(d) Streamlines – downstream rake.

Figure 1: Traditional post-processing techniques.

Velocity vectors struggle to cope with large velocity gradients as the required vector scaling can lead to overlapping or crossing vectors and/or insufficient resolution in separated regions. Vectors also have the added disadvantage of providing unintentional information about the underlying grid as they are conventionally presented at either nodes or cell centres. This can obscure flow features especially in solution-adapted computational results and may create artifacts or optical illusions in the output.

Figure 1(b) illustrates why contours of vorticity are not particularly useful in identifying vortical structure in separated flows as vorticity is concentrated in the wake shear layers and at flow boundaries. This would, therefore, require thresholding to reveal any wake vortices which may be present. Determination of appropriate thresholds is time-consuming if done interactively and may not reveal features if attempted automatically.

Streamlines can be independent of the underlying grid and give a continuous representation of the flow-field. However, as the lines follow the flow it is not easy to control their distribution throughout the field. Streamlines will tend to accumulate in certain areas and avoid others depending upon their start points. Figures 1(c) and 1(d) illustrate this by integrating streamlines forward and backward from a uniformly-spaced rake (shown in the figure). The position of the rake governs the effectiveness of the visualisation. In general a-priori knowledge of the flow-field is essential to optimise this type of plot, which may require interactive investigation and/or lead to the omission of features.

The sensitivity of streamlines to their start location makes them unsuitable for representation of transient datasets. The 'motion' of the flow-field relative to a fixed rake results in discontinuous animation frames. Both vectors and vorticity contours can be used to generate smooth animations but do not illustrate the convection and generation of vortical structures particularly well.

This paper will present two little-used post-processing techniques which, whilst not replacing the aforementioned techniques, do present the investigator with additional tools for data analysis and presentation. Both tools are suitable for use on two-dimensional computational and experimental datasets and require minimal user interaction during processing.

2   Line integral convolution

Line integral convolution (LIC) is a visualisation method which, when applied to fluid-dynamics vector fields, generates images reminiscent of long-exposure surface-tracer photographs of water flows. The basic technique was presented by Cabral and Leedom [1] as a computer graphics effect although they

realised it had application as a tool in vector field visualisation. The output of the process is essentially a high density streamline plot which clearly illustrates all the in-plane features of the input vector field.

2.1 Background

Figure 2 illustrates the input and output of the LIC technique as applied to a solid-body-rotation vector field. The basic process begins by combining a vector field, defined on a rectangular grid (Figure 2(b)), with an input image of the same resolution as the grid (Figure 2(a)). Each pixel, therefore, corresponds to one cell of the vector grid. At the first cell a streamline of a given length is integrated forward and backward using the vector field. The corresponding pixel in the output image is then assigned the mean intensity of the pixels lying under that streamline and the process is repeated at the next pixel/cell. As the calculation progresses, pixels on the same streamline are assigned similar intensities, resulting in the filtering, or smearing, of the input image along the streamlines of the vector field, see Figure 2(c).

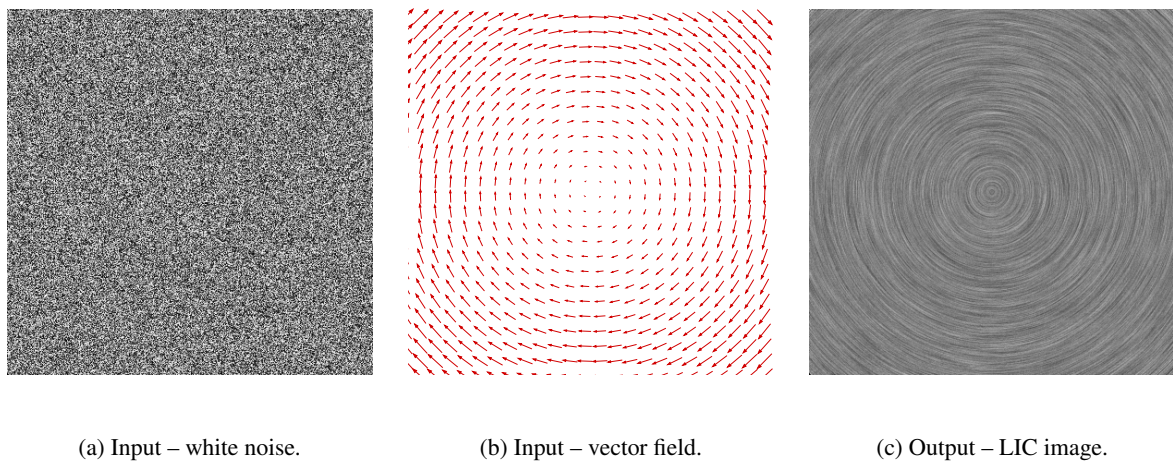| (a) Input – white noise. | (b) Input – vector field. | (c) Output – LIC image. |

Figure 2: Line integral convolution i/o.

The technique can be used to deform any input image along any vector field and is therefore a popular tool in computer graphics. For example, a suitable vector field can be used to add effects such as motion blur to a photograph. In fluid dynamics a white-noise input image is favoured as it results in an output image that is dominated by the vector data.

2.2 Current implementation

The LIC implementation used in this paper takes the basic approach of Cabral and Leedom [1] and extends it to include some of the useful features reported by subsequent investigators. Within each grid cell bilinear interpolation was used to evaluate vector values. The integration was performed using a 4th-order Runge-Kutta formula with an embedded 3rd-order formula allowing an adaptive step size to be used to maintain a given solution tolerance. In addition, the method provided an interpolant which enabled accurate transition between grid cells. The code was written in Fortran 90 with a Compaq Visual Fortan compiler. Although the implementation we have used is not particularly quick we have not felt it slow enough to warrant the implementation of a fast LIC technique such as that of Stalling and Hege [2].

2.2.1 Image enhancement

The LIC image shown in Figure 2(c) is again shown in Figure 3(a) to illustrate a process outlined by Okada and Kao [3] to improve the clarity of the output image, a process adopted in the current implementation. Using a constant vector field, the first LIC pass is carried out with a white noise input image. Subsequent passes use the output of the previous pass as their input. Additionally, the output of the second pass is sharpened to enhance the edges of the streamlines and then equalised to improve the overall contrast prior to its use in the final pass.
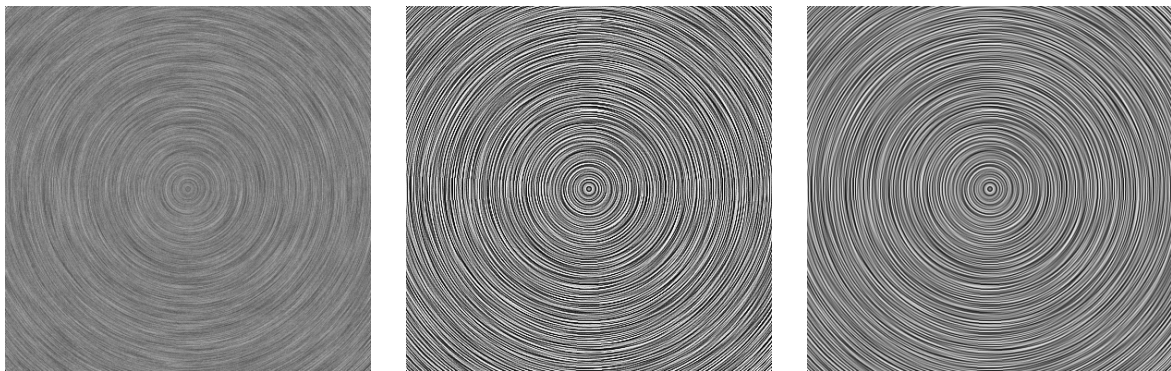
(a) 1st pass.   (b) 2nd pass (with sharpening   (c) 3rd pass.
                           and equalisation).

Figure 3: Improving clarity of line integral convolution.

2.2.2 Resolution independence

Stalling and Hege [2] suggested the use of interpolation to de-couple the resolutions of the input vector field and the output image. This allows the generation of high-resolution images from the sparse vector fields often encountered in experimental investigation. The current implementation uses natural neighbour interpolation for this over-sampling, the magnitude of which is restricted to integer values. Figure 4 illustrates the sensitivity of the process to over-sampling. The input dataset remained constant whilst the level of over-sampling was varied from 2 to 20. Although the size of the output image is dependent on the level of oversampling, to aid comparison, all images are shown at the same physical size. From the figure it can clearly be seen that over-sampling the grid up to twenty times has minimal effect on details such as vortex position, but further improves the clarity of the image.

2.2.3 Colouring

The images produced so far clearly convey the structures present in the vector field at the expense of direction and magnitude information. This can be addressed by colouring the LIC output by a scalar such as velocity angle [3] or pressure. It is equally possible to colour the LIC output to present features not represented by the streamlines such as shock waves or shear layers. An example of this is shown in Figure 5 using a computational simulation of supersonic flow ($M = 2$) around a 0.1 m diameter cylinder. Contours of density are used in the lower half of the image to accentuate the bow-shock whilst the LIC clearly shows the re-circulation in the near-wake.

3 Feature identification

The LIC technique presented in Section 2 is mainly a visualisation tool as it does not provide quantitative information about the flow structure (although it can be used to convey quantitative information through the use of colour and an appropriate legend). This section will present a technique based on the flow topology which can be used automatically to extract information, such as vortex centre positions, from the same planar datasets used in LIC.
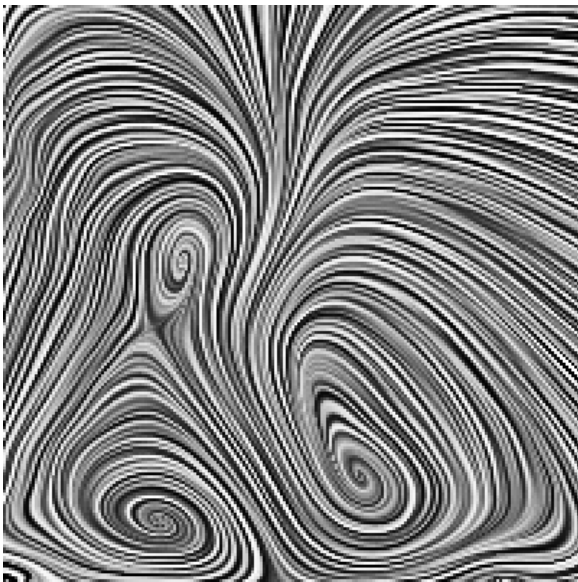
3.1 Background

The mathematical classification of fluid flow phenomena was comprehensively reported by Perry and Chong in both two and three-dimensions [4, 5]. Subsequently much work has been done in applying the
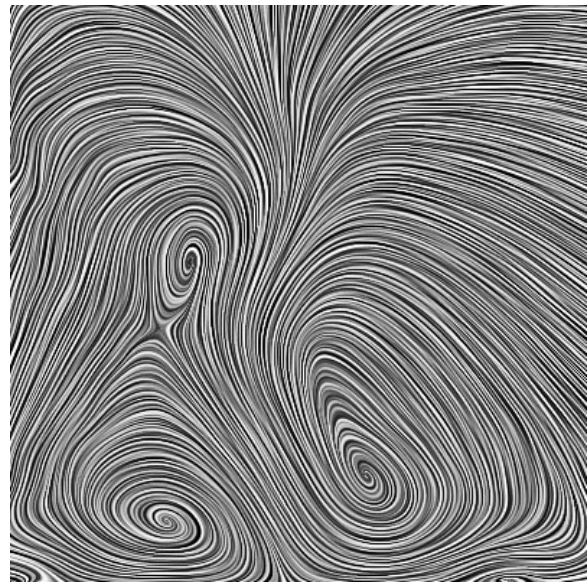
(a) 2× over-sampled.

(b) 5× over-sampled.

(c) 10× over-sampled.

(d) 20× over-sampled.

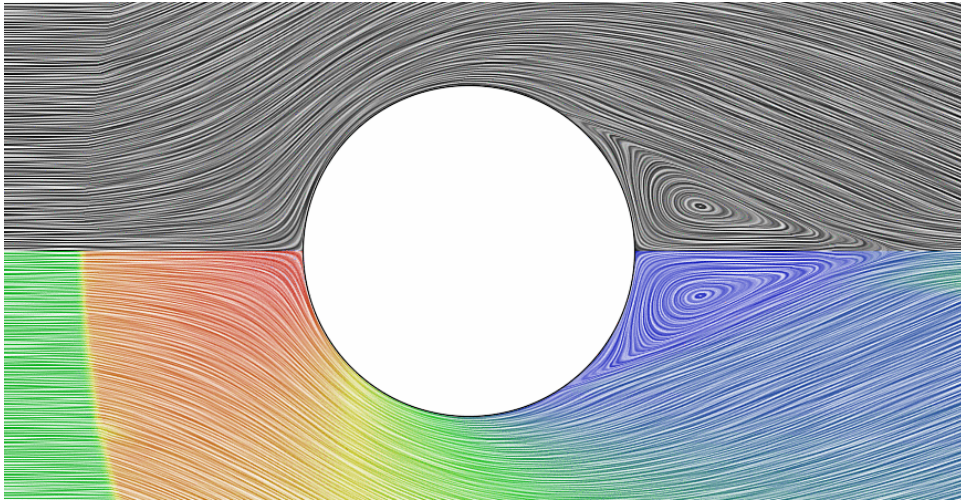Figure 4: Sensitivity of LIC to vector field over-sampling.

Figure 5: Coloured line integral convolution.

mathematics of topology to fluid mechanics in an attempt to develop a method to extract automatically flow features from CFD volumetric datasets. The identification of vortices has been a particular goal allowing the investigator to reduce a dataset to the vortices present within. The procedure has been complicated by the lack of an accepted mathematical definition of what constitutes a vortex, and accordingly many competing feature-extraction strategies have been proposed [6–9]. As such the application of critical point theory to two-dimensional planar datasets has been largely ignored by these investigators and does not appear to be widely applied. Calculation of vortex centre position does not suffer from the subjectivity associated with visual inspection of vector maps or LIC images.

3.2 Implementation

The procedure adopted for this paper comprised two stages, the first of which is the identification of all the critical points in the dataset. In the case of the planar datasets used previously, it is sufficient to isolate the points at which the two in-plane velocity components are zero. Each cell of the rectangular grid which contains a sign change in both velocity components is flagged as potentially containing a critical point. Bi-linear interpolation is then used to find whether a critical point does indeed exist within the cell. Figure 6 graphically illustrates this, showing a critical point at the intersection of the zero-contour lines of v (solid line) and w (broken line), with the surrounding flow visualised using streamlines.

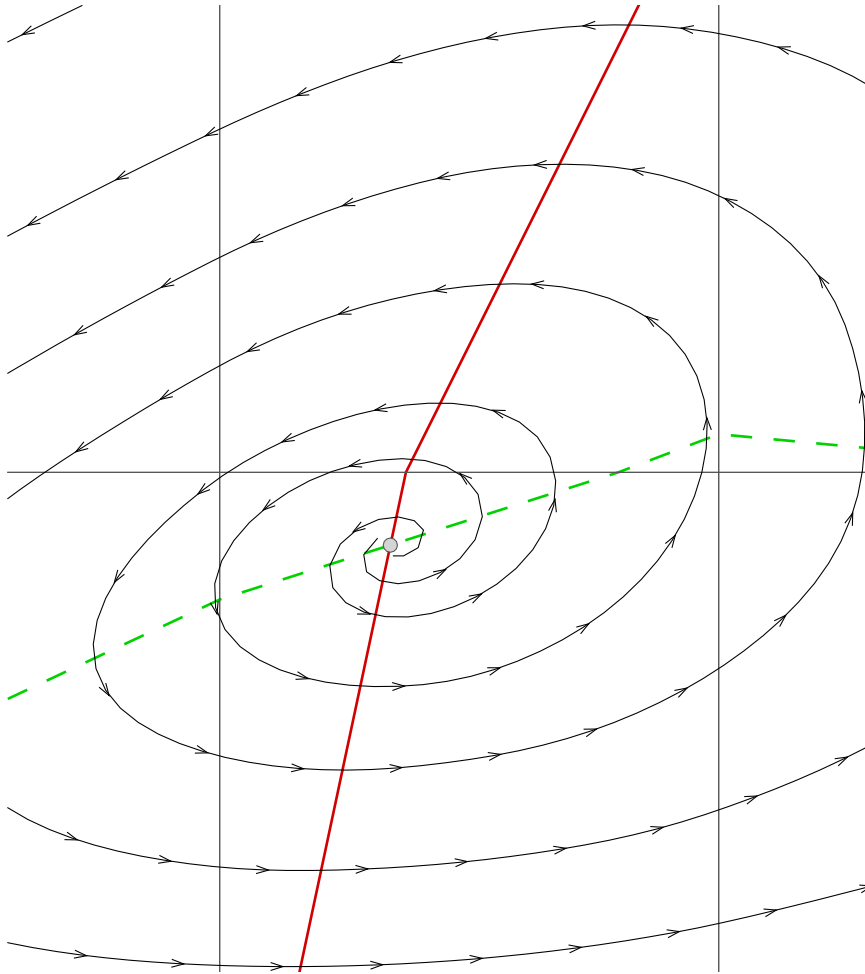Non-interactive classification of the identified critical points is the second phase of the procedure.

8

Figure 6: Critical point identification – focus source.

This separates vortices (also referred to as foci) from saddle points and the degenerate points (often found in PIV measurements) for visualisation and further analysis. The classification is based on the method detailed by Peikert [10] which uses properties of the point's Jacobian, ∇p (matrix of first partial derivatives) where;

$$\nabla p = \begin{bmatrix} p_{x,x} & p_{x,y} \\ p_{y,x} & p_{y,y} \end{bmatrix} \tag{1}$$

The properties of this matrix that are of particular interest are the negative trace, q, and the determinate, r, where:

$$q = -\left(p_{x,x} + p_{y,y}\right)$$
$$r = p_{x,x}\, p_{y,y} - p_{x,y}\, p_{y,x}$$

Table 1 outlines the evaluations made to determine from these two values the type of critical point under examination. This procedure has been deliberately limited to identification of foci and saddle points as they are most often investigated. It can easily be extended, however, to include node points or line features such as shear lines.

	$r > q^2/4$	$r < 0$
$q < 0$	focus source	saddle source
$q = 0$	centre	divergence free saddle
$q > 0$	focus sink	saddle sink

Table 1: Critical point classification.

It follows that this procedure can be used in three-dimensional datasets such as CFD by first extracting planes from the domain, a common practice when validating against experimental data. The procedure would, for example, allow an investigator to track the path of one or more trailing vortices as they are convected through the domain in a way not easily reproduced using streamlines.

4 Application

4.1 Circular cylinder in cross-flow

Figure 7 re-presents the streamline images from Figure 1 alongside the equivalent LIC image. The issue of missing features, caused by the streamline placement is avoided with LIC where both the downstream vortices, the saddle point and the upstream flow are all clearly visualised.
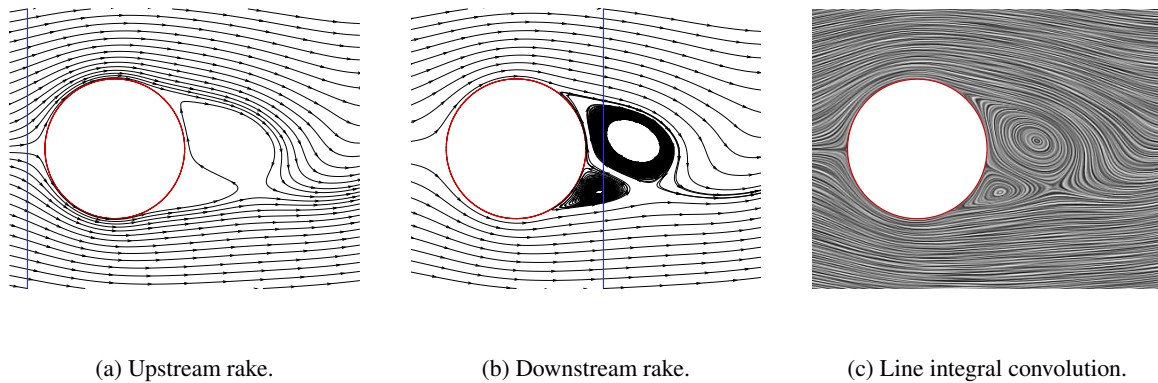

(a) Upstream rake.   (b) Downstream rake.   (c) Line integral convolution.

Figure 7: Comparison of streamline and LIC visualisations.

4.2 Animation

Whilst not directly part of the current implementation of LIC it is possible to produce informative animations from a sequence of LIC images. Figure 8 shows four frames from such an animation of a time-dependent CFD simulation of flow past a circular cylinder.

4.3 Cavity flows

Figure 9 illustrates the combination of the two techniques presented in this paper. In the background the flow-field in an open cavity is depicted using LIC applied to CFD data. The overlay shows the foci (circles) and saddle points (diamonds) along with the zero-contours of velocity used to identify them. The LIC clearly illustrates the small secondary flow present in the lower-left corner, likely to be missed by streamline visualisation. Application of either technique to consecutive frames of transient data would produce an informative animation and clearly show any variation in vortex centre position.
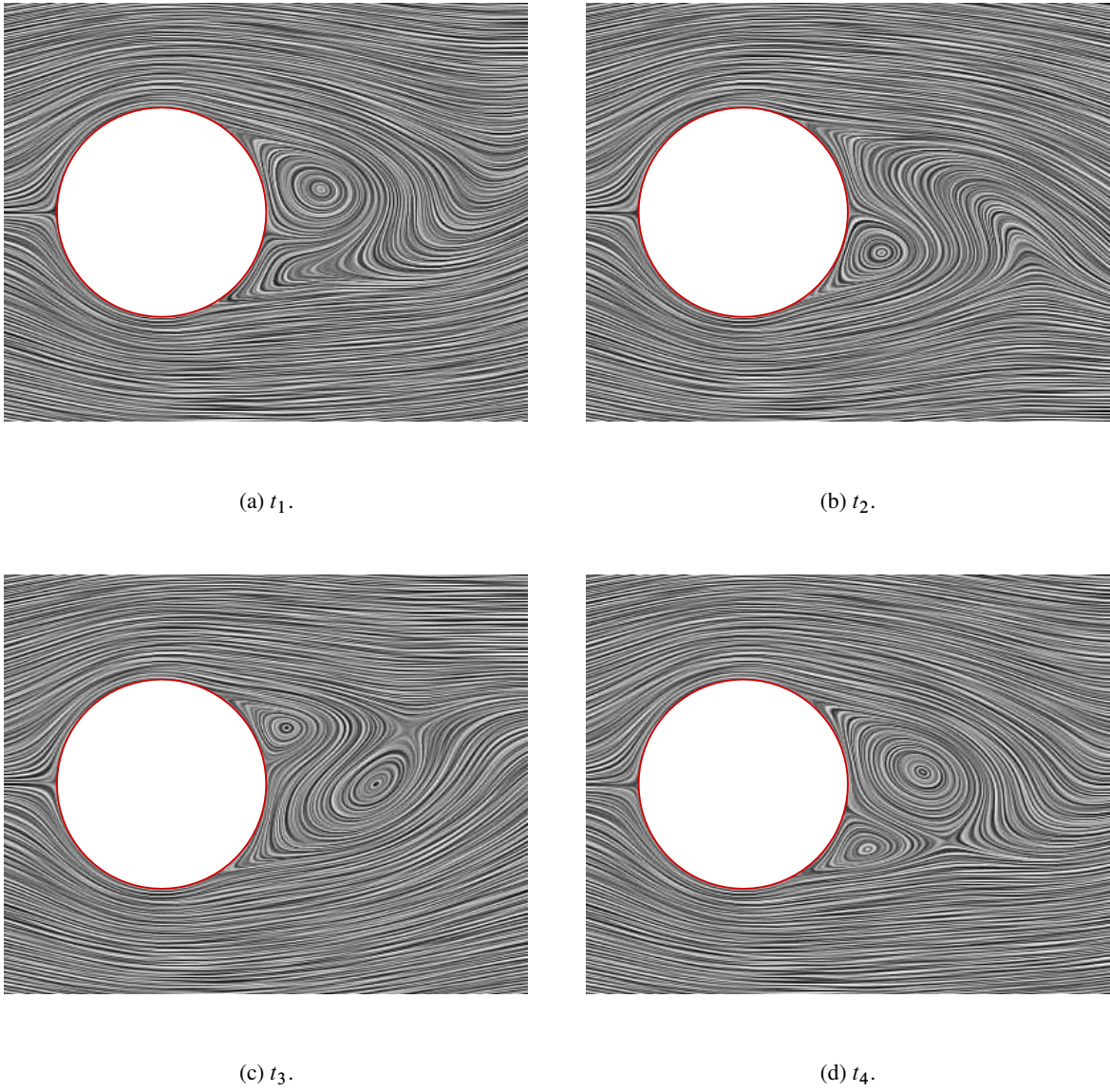
(a) t_1.

(b) t_2.

(c) t_3.

(d) t_4.

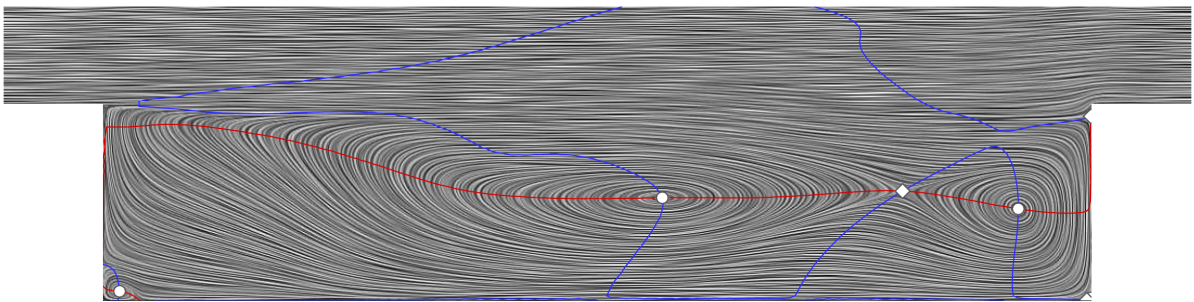Figure 8: Animation sequence.

Figure 9: Open cavity flow ($M_\infty = 0.85$, left-to-right freestream, off-centreline plane).

12

4.4 Three-dimensional, bluff-body wake

Figure 10 presents the results of a three-dimensional CFD simulation of the flow around a surface-mounted bluff body. Two contra-rotating vortices roll up from the upper shoulders of the body and are convected downstream. The downwash immediately behind the body and the relatively high velocity of the freestream make visualisation of the vortices using streamtubes difficult, see Figure 10(a). Figure 10(b) presents the same dataset reduced to only the vortex cores using the method described in Section 3. Each of the spheres in the image represents a critical point, in this case a focus, calculated from an extracted plane of data. This type of data reduction is particularly useful in identifying and/or visualising the interaction of vortices with downstream bodies, for example as found in the wake of racecar front wings.
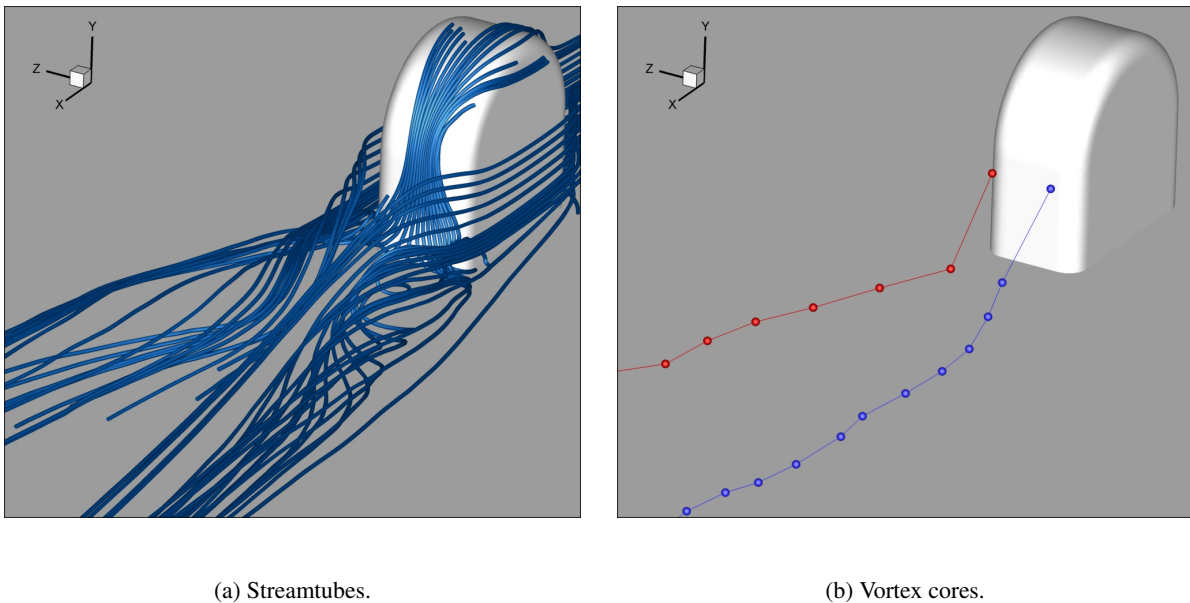

(a) Streamtubes.

(b) Vortex cores.

Figure 10: Trailing-vortex visualisation.

5 Conclusions

This paper has presented two over-looked post-processing techniques, line integral convolution and feature identification, which are not widely used in aerodynamic research. The techniques are mature and have been shown to be particularly useful tools in the visualisation and analysis of vortical flows. The operation and implementation of both techniques have been outlined along with their benefits, which

include:

- the two-dimensional, planar implementation renders the techniques equally applicable to experimental or computational datasets;

- no a-priori knowledge of the contents of the plane of interest is required to visualise and detect all features present;

- minimal user intervention.

The techniques were applied to a selection of diverse aerodynamic flows, with the output used to illustrate their capabilities.

6 Acknowledgements

References

[1] B. Cabral and L.C. Leedom. Imaging vector fields using line integral convolution. In *Proceedings of the 20th Annual Conference on Computer Graphics and Interactive Techniques, SIGGRAPH '93*, pages 263–270, Anaheim, CA, USA, 2-6 August 1993.

[2] D. Stalling and H-C. Hege. Fast and resolution independent line integral convolution. In *Proceedings of the 22nd Annual Conference on Computer Graphics and Interactive Techniques, SIGGRAPH '95*, pages 249–256, Los Angeles, CA, USA, 6-11 August 1995.

[3] A. Okada and D. Kao. Enhanced line integral convolution with flow feature detection. In G. G. Grinstein and R. F. Erbacher, editors, *Proceedings of SPIE: Visual Data Exploration and Analysis IV*, volume 3017, pages 206–217, San Jose, CA, USA, 8-12 February 1997.

[4] A. E. Perry and M. S. Chong. A description of eddying motions and flow patterns using critical-point concepts. *Annual Review of Fluid Mechanics*, 19(1):125–155, 1987.

[5] M. S. Chong, A. E. Perry, and B. J. Cantwell. A general classification of three-dimensional flow fields. *Physics of Fluids A*, 2(5):765–777, 1990.

[6] Y. Levy, D. Degani, and A. Seginer. Graphical visualisation of vortical flows by means of helicity. *AIAA Journal*, 28(8):1347–1352, August 1990.

[7] D. C. Banks and B. A. Singer. Vortex tubes in turbulent flows: Identification, representation, reconstruction. In *Proceedings of the IEEE Conference on Visualization*, pages 132–139, Washington, DC, USA, 17-21 October 1994.

[8] D. Sujudi and R. Haimes. Identification of swirling flow in 3-d vector fields. Technical report, Dept. Aeronautics and Astronautics, MIT, Cambridge, MA, USA, 1995.

[9] R. Peikert and M. Roth. The parallel vectors operator – a vector field visualization primitive. In *Proceedings of the IEEE Conference on Visualization*, pages 263–270, San Francisco, CA, USA, 24-29 October 1999.

[10] R. Peikert. Linear 2-d vector fields. http://graphics.ethz.ch/ peikert/personal/Linear2D.

[11] S. A. Ritchie, K. Knowles, and N. J. Lawson. Characterisation of a 3-d l/h = 5 cavity flow at transonic speeds using experimental and numerical methods. In *Proceedings of the 2nd International Symposium on Integrating CFD and Experiments in Aerodynamics*, Shrivenham, UK, 5-6 September 2005.